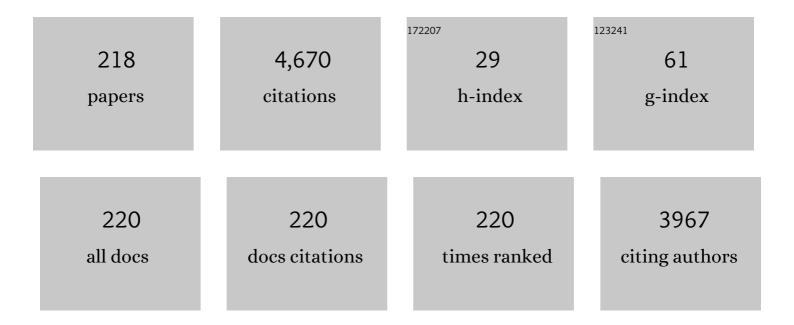
List of Publications by Year in descending order

Source: https://exaly.com/author-pdf/6856145/publications.pdf Version: 2024-02-01



#	Article	IF	CITATIONS
1	A versatile wavelet domain noise filtration technique for medical imaging. IEEE Transactions on Medical Imaging, 2003, 22, 323-331.	5.4	450
2	Hyperspectral and LiDAR Data Fusion: Outcome of the 2013 GRSS Data Fusion Contest. IEEE Journal of Selected Topics in Applied Earth Observations and Remote Sensing, 2014, 7, 2405-2418.	2.3	349
3	Estimating the probability of the presence of a signal of interest in multiresolution single- and multiband image denoising. IEEE Transactions on Image Processing, 2006, 15, 654-665.	6.0	328
4	A joint inter- and intrascale statistical model for Bayesian wavelet based image denoising. IEEE Transactions on Image Processing, 2002, 11, 545-557.	6.0	228
5	Processing of Multiresolution Thermal Hyperspectral and Digital Color Data: Outcome of the 2014 IEEE GRSS Data Fusion Contest. IEEE Journal of Selected Topics in Applied Earth Observations and Remote Sensing, 2015, 8, 2984-2996.	2.3	193
6	Semisupervised Local Discriminant Analysis for Feature Extraction in Hyperspectral Images. IEEE Transactions on Geoscience and Remote Sensing, 2013, 51, 184-198.	2.7	152
7	Context-Aware Patch-Based Image Inpainting Using Markov Random Field Modeling. IEEE Transactions on Image Processing, 2015, 24, 444-456.	6.0	133
8	Generalized Graph-Based Fusion of Hyperspectral and LiDAR Data Using Morphological Features. IEEE Geoscience and Remote Sensing Letters, 2015, 12, 552-556.	1.4	129
9	A Review of Wavelet Denoising in MRI and Ultrasound Brain Imaging. Current Medical Imaging, 2006, 2, 247-260.	0.4	100
10	Deep Feature Fusion via Two-Stream Convolutional Neural Network for Hyperspectral Image Classification. IEEE Transactions on Geoscience and Remote Sensing, 2020, 58, 2615-2629.	2.7	95
11	The effect of Gibbs ringing artifacts on measures derived from diffusion MRI. NeuroImage, 2015, 120, 441-455.	2.1	94
12	Classification of Hyperspectral Data Over Urban Areas Using Directional Morphological Profiles and Semi-Supervised Feature Extraction. IEEE Journal of Selected Topics in Applied Earth Observations and Remote Sensing, 2012, 5, 1177-1190.	2.3	91
13	Hyperspectral Unmixing Using Double Reweighted Sparse Regression and Total Variation. IEEE Geoscience and Remote Sensing Letters, 2017, 14, 1146-1150.	1.4	85
14	Crack detection and inpainting for virtual restoration of paintings: The case of the Ghent Altarpiece. Signal Processing, 2013, 93, 605-619.	2.1	77
15	Fusion of pixel and object-based features for weed mapping using unmanned aerial vehicle imagery. International Journal of Applied Earth Observation and Geoinformation, 2018, 67, 43-53.	1.4	76
16	Wavelet-Domain Video Denoising Based on Reliability Measures. IEEE Transactions on Circuits and Systems for Video Technology, 2006, 16, 993-1007.	5.6	75
17	Multiscale Superpixel-Level Subspace-Based Support Vector Machines for Hyperspectral Image Classification. IEEE Geoscience and Remote Sensing Letters, 2017, 14, 2142-2146.	1.4	68
18	An integrated method of adaptive enhancement for unsupervised segmentation of MRI brain images. Pattern Recognition Letters, 2003, 24, 2549-2560.	2.6	63

#	Article	IF	CITATIONS
19	Multiresolution Denoising for Optical Coherence Tomography: A Review and Evaluation. Current Medical Imaging, 2008, 4, 270-284.	0.4	57
20	Iterative CT Reconstruction Using Shearlet-Based Regularization. IEEE Transactions on Nuclear Science, 2013, 60, 3305-3317.	1.2	55
21	Removal of Correlated Noise by Modeling the Signal of Interest in the Wavelet Domain. IEEE Transactions on Image Processing, 2009, 18, 1153-1165.	6.0	54
22	Extending the Depth of Field in Microscopy Through Curvelet-Based Frequency-Adaptive Image Fusion. , 2007, , .		45
23	Rate Allocation Algorithm for Pixel-Domain Distributed Video Coding Without Feedback Channel. , 2007, , .		44
24	Combined Wavelet-Domain and Motion-Compensated Video Denoising Based on Video Codec Motion Estimation Methods. IEEE Transactions on Circuits and Systems for Video Technology, 2009, 19, 417-421.	5.6	42
25	A New Fuzzy-Based Wavelet Shrinkage Image Denoising Technique. Lecture Notes in Computer Science, 2006, , 12-23.	1.0	37
26	Supervised feature-based classification of multi-channel SAR images. Pattern Recognition Letters, 2006, 27, 252-258.	2.6	36
27	Image Denoising Using Mixtures of Projected Gaussian Scale Mixtures. IEEE Transactions on Image Processing, 2009, 18, 1689-1702.	6.0	36
28	Combined wavelet domain and temporal video denoising. , 0, , .		35
29	Augmented Lagrangian based reconstruction of non-uniformly sub-Nyquist sampled MRI data. Signal Processing, 2011, 91, 2731-2742.	2.1	35
30	Double reweighted sparse regression for hyperspectral unmixing. , 2016, , .		35
31	Brain blood vessel segmentation using line-shaped profiles. Physics in Medicine and Biology, 2013, 58, 8041-8061.	1.6	34
32	Noise estimation for video processing based on spatio-temporal gradients. IEEE Signal Processing Letters, 2006, 13, 337-340.	2.1	32
33	Context adaptive image denoising through modeling of curvelet domain statistics. Journal of Electronic Imaging, 2008, 17, 033021.	0.5	30
34	Denoising of multicomponent images using wavelet least-squares estimators. Image and Vision Computing, 2008, 26, 1038-1051.	2.7	28
35	Digital Image Processing of The Ghent Altarpiece: Supporting the painting's study and conservation treatment. IEEE Signal Processing Magazine, 2015, 32, 112-122.	4.6	28
36	Fusion of Spectral and Spatial Information for Classification of Hyperspectral Remote-Sensed Imagery by Local Graph. IEEE Journal of Selected Topics in Applied Earth Observations and Remote Sensing, 2016, 9, 583-594.	2.3	27

#	Article	IF	CITATIONS
37	Overview of the Whole Heart and Heart Chamber Segmentation Methods. Cardiovascular Engineering and Technology, 2020, 11, 725-747.	0.7	24
38	A GPU-Accelerated Real-Time NLMeans Algorithm for Denoising Color Video Sequences. Lecture Notes in Computer Science, 2010, , 46-57.	1.0	24
39	Video Denoising Using Multiple Class Averaging with Multiresolution. Lecture Notes in Computer Science, 2003, , 172-179.	1.0	23
40	Skeletonization method for vessel delineation of arteriovenous malformation. Computers in Biology and Medicine, 2018, 93, 93-105.	3.9	23
41	Semisupervised Sparse Subspace Clustering Method With a Joint Sparsity Constraint for Hyperspectral Remote Sensing Images. IEEE Journal of Selected Topics in Applied Earth Observations and Remote Sensing, 2019, 12, 989-999.	2.3	23
42	Noise reduction in video sequences using wavelet-domain and temporal filtering. , 2004, 5266, 48.		22
43	An overview of stateâ€ofâ€theâ€art image restoration in electron microscopy. Journal of Microscopy, 2018, 271, 239-254.	0.8	22
44	Fuzzy logic-based approach to wavelet denoising of 3D images produced by time-of-flight cameras. Optics Express, 2010, 18, 22651.	1.7	21
45	Two-stage fusion of thermal hyperspectral and visible RGB image by PCA and guided filter. , 2015, , .		21
46	A Robust Sparse Representation Model for Hyperspectral Image Classification. Sensors, 2017, 17, 2087.	2.1	21
47	Left atrial appendage segmentation from 3D CCTA images for occluder placement procedure. Computers in Biology and Medicine, 2019, 104, 163-174.	3.9	21
48	Despeckling SAR images using wavelets and a new class of adaptive shrinkage estimators. , 0, , .		20
49	Wavelet Domain Image Denoising for Non-Stationary Noise and Signal-Dependent Noise. , 2006, , .		20
50	Generalized pixel profiling and comparative segmentation with application to arteriovenous malformation segmentation. Medical Image Analysis, 2012, 16, 991-1002.	7.0	20
51	Crack Detection in Paintings Using Convolutional Neural Networks. IEEE Access, 2020, 8, 74535-74552.	2.6	20
52	Fuzzy logic recursive motion detection and denoising of video sequences. Journal of Electronic Imaging, 2006, 15, 023008.	0.5	19
53	Efficient design of a low redundant Discrete Shearlet Transform. , 2009, , .		19
54	Joint photometric and geometric image registration in the total least square sense. Pattern Recognition Letters, 2011, 32, 2061-2067.	2.6	19

#	Article	IF	CITATIONS
55	Recursive temporal denoising and motion estimation of video. , 0, , .		18
56	Vehicle matching in smart camera networks using image projection profiles at multiple instances. Image and Vision Computing, 2013, 31, 673-685.	2.7	18
5 <b>7</b>	Subspace Clustering for Hyperspectral Images via Dictionary Learning With Adaptive Regularization. IEEE Transactions on Geoscience and Remote Sensing, 2022, 60, 1-17.	2.7	18
58	Video denoising by fuzzy motion and detail adaptive averaging. Journal of Electronic Imaging, 2008, 17, 043005.	0.5	17
59	Joint Sparsity Based Sparse Subspace Clustering for Hyperspectral Images. , 2018, , .		17
60	Realistic camera noise modeling with application to improved HDR synthesis. Eurasip Journal on Advances in Signal Processing, 2012, 2012, .	1.0	16
61	Hyperspectral image deblurring with PCA and total variation. , 2013, , .		16
62	Obstacle detection for pedestrians with a visual impairment based on 3D imaging. , 2013, , .		15
63	A Robust Dynamic Classifier Selection Approach for Hyperspectral Images with Imprecise Label Information. Sensors, 2020, 20, 5262.	2.1	15
64	Virtual Restoration of the Ghent Altarpiece Using Crack Detection and Inpainting. Lecture Notes in Computer Science, 2011, , 417-428.	1.0	14
65	A fast iterative kernel PCA feature extraction for hyperspectral images. , 2010, , .		13
66	Object Tracking Using Naive Bayesian Classifiers. Lecture Notes in Computer Science, 2008, , 775-784.	1.0	13
67	Classification of Hyperspectral Data over Urban Areas Based on Extended Morphological Profile with Partial Reconstruction. Lecture Notes in Computer Science, 2012, , 278-289.	1.0	13
68	Compass: a joint framework for Parallel Imaging and Compressive Sensing in MRI. , 2010, , .		12
69	Combining feature fusion and decision fusion for classification of hyperspectral and LiDAR data. , 2014, , .		12
70	Split-and-match: A Bayesian framework for vehicle re-identification in road tunnels. Engineering Applications of Artificial Intelligence, 2015, 45, 220-233.	4.3	12
71	Sketch-Based Subspace Clustering of Hyperspectral Images. Remote Sensing, 2020, 12, 775.	1.8	12
72	Non-Overlapping Multi-camera Detection and Tracking of Vehicles in Tunnel Surveillance. , 2011, , .		11

#	Article	IF	CITATIONS
73	Sparse Recovery in Magnetic Resonance Imaging With a Markov Random Field Prior. IEEE Transactions on Medical Imaging, 2017, 36, 2104-2115.	5.4	11
74	D-BRAIN: Anatomically Accurate Simulated Diffusion MRI Brain Data. PLoS ONE, 2016, 11, e0149778.	1.1	11
75	A wavelet-based image denoising technique using spatial priors. , 0, , .		10
76	Passive Error Concealment for Wavelet-Coded I-Frames With an Inhomogeneous Gauss–Markov Random Field Model. IEEE Transactions on Image Processing, 2009, 18, 783-796.	6.0	10
77	Automatic 3D graph cuts for brain cortex segmentation in patients with focal cortical dysplasia. , 2011, 2011, 7981-4.		10
78	Feature extraction for hyperspectral images based on semi-supervised local discriminant analysis. , 2011, , .		10
79	3D MICROWAVE TOMOGRAPHY WITH HUBER REGULARIZATION APPLIED TO REALISTIC NUMERICAL BREAST PHANTOMS. Progress in Electromagnetics Research, 2016, 155, 75-91.	1.6	10
80	Hybrid-Hypergraph Regularized Multiview Subspace Clustering for Hyperspectral Images. IEEE Transactions on Geoscience and Remote Sensing, 2022, 60, 1-16.	2.7	10
81	Spectral Feature Fusion Networks With Dual Attention for Hyperspectral Image Classification. IEEE Transactions on Geoscience and Remote Sensing, 2022, 60, 1-14.	2.7	10
82	Heterogeneous Regularization-Based Tensor Subspace Clustering for Hyperspectral Band Selection. IEEE Transactions on Neural Networks and Learning Systems, 2023, 34, 9259-9273.	7.2	10
83	Fuzzy logic recursive change detection for tracking and denoising of video sequences. , 2005, 5685, 771.		9
84	Reduced decoder complexity and latency in pixel-domain Wyner–Ziv video coders. Signal, Image and Video Processing, 2008, 2, 129-140.	1.7	9
85	Robust segmentation methods with an application to aortic pulse wave velocity calculation. Computerized Medical Imaging and Graphics, 2014, 38, 179-189.	3.5	9
86	Hyperspectral unmixing by reweighted low rank and total variation. , 2016, , .		9
87	Information-Theoretic Analysis of Dependencies Between Curvelet Coefficients. , 2006, , .		8
88	Locally Adaptive Passive Error Concealment for Wavelet Coded Images. IEEE Signal Processing Letters, 2008, 15, 178-181.	2.1	8
89	Segmentation and length measurement of the abdominal blood vessels in 3-D MRI images. , 2009, 2009, 4399-402.		8
90	A Structural Subspace Clustering Approach for Hyperspectral Band Selection. IEEE Transactions on Geoscience and Remote Sensing, 2022, 60, 1-15.	2.7	8

#	Article	IF	CITATIONS
91	FPCA Design and Implementation of a Wavelet-Domain Video Denoising System. Lecture Notes in Computer Science, 2005, , 650-657.	1.0	7
92	Wavelet domain denoising of multispectral remote sensing imagery adapted to the local spatial and spectral context. , 0, , .		7
93	A Bayesian formulation of edge-stopping functions in nonlinear diffusion. IEEE Signal Processing Letters, 2006, 13, 501-504.	2.1	7
94	Machine vision detection of isolated and overlapped nematode worms using skeleton analysis. , 2008, ,		7
95	Optimization of Packetization Masks for Image Coding Based on an Objective Cost Function for Desired Packet Spreading. IEEE Transactions on Image Processing, 2008, 17, 1849-1863.	6.0	7
96	Segmentation of brain blood vessels using projections in 3-D CT angiography images. , 2011, 2011, 8475-8.		7
97	A primal-dual algorithm for joint demosaicking and deconvolution. , 2012, , .		7
98	Computationally Efficient Locally Adaptive Demosaicing of Color Filter Array Images Using the Dual-Tree Complex Wavelet Packet Transform. PLoS ONE, 2013, 8, e61846.	1.1	7
99	Group Convolutional Neural Networks for Hyperspectral Image Classification. , 2019, , .		7
100	Improved Pixel-Based Rate Allocation for Pixel-Domain Distributed Video Coders Without Feedback Channel. , 2007, , 663-674.		7
101	Image de-noising in the wavelet domain using prior spatial constraints. , 1999, , .		7
102	Wavelet based denoising techniques for ultrasound images. , 0, , .		6
103	A Bayesian approach to nonlinear diffusion based on a Laplacian prior for ideal image gradient. , 2005, , $\cdot$		6
104	A Distributed Coding-Based Extension of a Mono-View to a Multi-View Video System. , 2007, , .		6
105	Removal of Correlated Noise by Modeling Spatial Correlations and Interscale Dependencies in the Complex Wavelet Domain. Proceedings International Conference on Image Processing, 2007, , .	0.0	6
106	Combined non-local and multi-resolution sparsity prior in image restoration. , 2012, , .		6
107	Iterative CT reconstruction using shearlet-based regularization. , 2012, , .		6
108	Multimodal Target Detection by Sparse Coding: Application to Paint Loss Detection in Paintings. IEEE Transactions on Image Processing, 2020, 29, 7681-7696.	6.0	6

4

#	Article	IF	CITATIONS
109	Design of a tight frame of 2D shearlets based on a fast non-iterative analysis and synthesis algorithm. Proceedings of SPIE, 2011, , .	0.8	6
110	Automatic Individual Detection and Separation of Multiple Overlapped Nematode Worms Using Skeleton Analysis. Lecture Notes in Computer Science, 2008, , 817-826.	1.0	6
111	Improved segmentation of ultrasound brain tissue incorporating expert evaluation. , 2005, 2005, 6480-3.		5
112	Locally adaptive complex wavelet-based demosaicing for color filter array images. , 2009, , .		5
113	Single-image super-resolution using sparsity constraints and non-local similarities at multiple resolution scales. Proceedings of SPIE, 2010, , .	0.8	5
114	Training neural networks on artificially generated data: a novel approach to SAR speckle removal. International Journal of Remote Sensing, 2011, 32, 3405-3425.	1.3	5
115	Markov Random Field based image inpainting with context-aware label selection. , 2012, , .		5
116	Object identification by using orthonormal circus functions from the trace transform. , 2012, , .		5
117	Neighborhood-consensus message passing as a framework for generalized iterated conditional expectations. Pattern Recognition Letters, 2012, 33, 309-318.	2.6	5
118	Efficient foreground detection for realâ€ŧime surveillance applications. Electronics Letters, 2013, 49, 1143-1145.	0.5	5
119	Acoustic Seafloor Classification Using the Weyl Transform of Multibeam Echosounder Backscatter Mosaic. Remote Sensing, 2021, 13, 1760.	1.8	5
120	On Hybrid Directional Transform-Based Intra-band Image Coding. Lecture Notes in Computer Science, 2007, , 1049-1060.	1.0	5
121	Surface Reconstruction of Wear in Carpets by Using a Wavelet Edge Detector. Lecture Notes in Computer Science, 2010, , 309-320.	1.0	5
122	Wavelet-based denoising for 3D OCT images. Proceedings of SPIE, 2007, 6696, 254.	0.8	4
123	Combinedwavelet Domain and Motion Compensated Filtering Compliant with Video Codecs. , 2007, , .		4
124	Analysis of the Statistical Dependencies in the Curvelet Domain and Applications in Image Compression. Lecture Notes in Computer Science, 2007, , 1061-1071.	1.0	4
125	Wavelet Based Joint Denoising of Depth and Luminance Images. , 2007, , .		4

126 Image blur estimation based on the average cone of ratio in the wavelet domain. , 2009, , .

#	Article	IF	CITATIONS
127	Robust Detection and Tracking of Moving Objects in Traffic Video Surveillance. Lecture Notes in Computer Science, 2009, , 494-505.	1.0	4
128	A Recursive Scheme for Computing Autocorrelation Functions of Decimated Complex Wavelet Subbands. IEEE Transactions on Signal Processing, 2010, 58, 3907-3912.	3.2	4
129	On structured sparsity and selected applications in tomographic imaging. Proceedings of SPIE, 2011, , .	0.8	4
130	Texture and color descriptors as a tool for context-aware patch-based image inpainting. , 2012, , .		4
131	Total least square kernel regression. Journal of Visual Communication and Image Representation, 2012, 23, 94-99.	1.7	4
132	Suppression of Correlated Noise. , 0, , .		4
133	Virtual restoration of paintings based on deep learning. , 2022, , .		4
134	Recent Progress in Epicardial and Pericardial Adipose Tissue Segmentation and Quantification Based on Deep Learning: A Systematic Review. Applied Sciences (Switzerland), 2022, 12, 5217.	1.3	4
135	Locally Adaptive Intrasubband Interpolation of Lost Lowfrequency Coefficients Inwavelet Coded Images. , 2007, , .		3
136	EM-based estimation of spatially variant correlated image noise. , 2008, , .		3
137	Spatiogram features to characterize pearls in paintings. , 2011, , .		3
138	Wavelet-Based Analysis and Estimation of Colored Noise. , 0, , .		3
139	Efficient multiscale and multidirectional representation of 3D data using the 3D discrete shearlet transform. , 2011, , .		3
140	Real-time vehicle matching for multi-camera tunnel surveillance. , 2011, , .		3
141	Quantitative microwave tomography from sparse measurements using a robust huber regularizer. , 2012, , .		3
142	Centerline calculation for extracting abdominal aorta in 3-D MRI images. , 2012, 2012, 3982-5.		3
143	Image projection clues for improved real-time vehicle tracking in tunnels. Proceedings of SPIE, 2012, , .	0.8	3
144	Complex wavelet joint denoising and demosaicing using Gaussian scale mixtures. , 2013, , .		3

9

#	Article	IF	CITATIONS
145	Weakly Convex Discontinuity Adaptive Regularization for Microwave Imaging. IEEE Transactions on Antennas and Propagation, 2013, 61, 6242-6246.	3.1	3
146	Automatic High-Bandwidth Calibration and Reconstruction of Arbitrarily Sampled Parallel MRI. PLoS ONE, 2014, 9, e98937.	1.1	3
147	Depth-guided patch-based disocclusion filling for view synthesis via Markov random field modelling. , 2014, , .		3
148	Skeleton calculation for automatic extraction of arteriovenous malformation in 3-D CTA images. , 2014, , .		3
149	Weakly convex discontinuity adaptive regularization for 3D quantitative microwave tomography. Inverse Problems, 2014, 30, 085005.	1.0	3
150	Deep Learning for Paint Loss Detection with a multiscale, translation invariant network. , 2019, , .		3
151	Accelerating in vivo fast spin echo high angular resolution diffusion imaging with an isotropic resolution in mice through compressed sensing. Magnetic Resonance in Medicine, 2021, 85, 1397-1413.	1.9	3
152	Fully Group Convolutional Neural Networks for Robust Spectral–Spatial Feature Learning. IEEE Transactions on Geoscience and Remote Sensing, 2022, 60, 1-14.	2.7	3
153	A New Fuzzy Motion and Detail Adaptive Video Filter. Lecture Notes in Computer Science, 2007, , 640-651.	1.0	3
154	Noise Removal from Images by Projecting onto Bases of Principal Components. , 2007, , 190-199.		3
155	A deep learning approach to crack detection on road surfaces. , 2020, , .		3
156	A new restoration method and its application to speckle images. , 0, , .		2
157	A novel method for adaptive enhancement and unsupervised segmentation of MRI brain image. , 0, , .		2
158	Combining multivariate statistics and speckle reduction for line detection in multichannel SAR images. , 2004, , .		2
159	Multiscale statistical image models and Bayesian methods. , 2004, 5266, 60.		2
160	Spatio-Temporal Approach for Noise Estimation. , 0, , .		2
161	Spatially adaptive image denoising based on joint image statistics in the curvelet domain. , 2006, 6383, 158.		2
162	Content adaptive wavelet based method for joint denoising of depth and luminance images. Proceedings of SPIE, 2007, , .	0.8	2

#	ARTICLE	IF	CITATIONS
163	A Distributed Coding-Based Content-Aware Multi-View Video System. , 2007, , .		2
164	Efficient video segmentation using temporally updated mean shift clustering. Proceedings of SPIE, 2008, , .	0.8	2
165	A filter design technique for improving the directional selectivity of the first scale of the Dual-Tree complex wavelet transform. , 2009, , .		2
166	Segmentation of airways in lungs using projections in 3-D CT angiography images. , 2010, 2010, 3162-5.		2
167	Reconstruction of High Dynamic Range images with poisson noise modeling and integrated denoising. , 2011, , .		2
168	Neighbourhood-consensus message passing and its potentials in image processing applications. Proceedings of SPIE, 2011, , .	0.8	2
169	A mathematical morphology-based approach for vehicle detection in road tunnels. Proceedings of SPIE, 2011, , .	0.8	2
170	Denoising algorithm for the 3D depth map sequences based on multihypothesis motion estimation. Eurasip Journal on Advances in Signal Processing, 2011, 2011, .	1.0	2
171	Two-stage denoising method for hyperspectral images combining KPCA and total variation. , 2013, , .		2
172	Pixel profiling for extraction of arteriovenous malformation in 3-D CTA images. , 2014, , .		2
173	A Deep Learning-Based Approach for Defect Detection and Removing on Archival Photos. IS&T International Symposium on Electronic Imaging, 2020, 2020, 29-1-29-7.	0.3	2
174	HYPERSPECTRAL IMAGE KERNEL SPARSE SUBSPACE CLUSTERING WITH SPATIAL MAX POOLING OPERATION. International Archives of the Photogrammetry, Remote Sensing and Spatial Information Sciences - ISPRS Archives, 0, XLI-B3, 945-948.	0.2	2
175	Class Reconstruction Driven Adversarial Domain Adaptation for Hyperspectral Image Classification. Lecture Notes in Computer Science, 2019, , 472-484.	1.0	2
176	<title>Real-time wavelet domain video denoising implemented in FPGA</title> . , 2004, , .		1
177	Wavelet-based stereo images reconstruction using depth images. , 2007, 6701, 813.		1
178	Watershed data aggregation for mean-shift video segmentation. , 2007, , .		1
179	Bayesian wavelet-based denoising of multicomponent images. Proceedings of SPIE, 2007, , .	0.8	1

180 Real-time wavelet based blur estimation on cell BE platform. , 2010, , .

1

#	Article	IF	CITATIONS
181	Consistent joint photometric and geometric image registration. , 2010, , .		1
182	Classification of multi-source images using color morphological profiles. , 2011, , .		1
183	Advanced statistical tools for enhanced quality digital imaging with realistic capture models. Eurasip Journal on Advances in Signal Processing, 2013, 2013, .	1.0	1
184	A split-augmented Lagrangian algorithm for spectral factorization of a set of 2D directional filters and application to the design of compact shearlet frames. Proceedings of SPIE, 2013, , .	0.8	1
185	New insights in Huber and TV-like regularizers in microwave imaging. , 2013, , .		1
186	Compressed Sensing using sparse binary measurements: A rateless coding perspective. , 2015, , .		1
187	Compressed sensing in MRI with a Markov random field prior for spatial clustering of subband coefficients. , 2016, , .		1
188	Achievability of the rate-distortion function in binary uniform source coding with side information. , 2016, , .		1
189	A comparison on multiple level features for fusion of hyperspectral and LiDAR data. , 2017, , .		1
190	Robust joint sparsity model for hyperspectral image classification. , 2017, , .		1
191	Landmark-Based Large-Scale Sparse Subspace Clustering Method for Hyperspectral Images. , 2019, , .		1
192	Hierarchical Variational Autoencoders For Visual Counterfactuals. , 2021, , .		1
193	Efficient Local Image Descriptors Learned With Autoencoders. IEEE Access, 2022, 10, 221-235.	2.6	1
194	Detecting variable source areas from temporal radar imagery using advanced image enhancement techniques. , 0, , .		0
195	Wavelet-based joint video de-interlacing and denoising. , 2006, 6383, 147.		0
196	Locally adaptive reconstruction of lost low-frequency coefficients in wavelet coded images. , 2007, , .		0
197	Classifying electrocardiogram peaks using newwavelet domain features. , 2008, , .		0
198	Locally adaptive passive error concealment for wavelet coded video. , 2009, , .		0

#	Article	IF	CITATIONS
199	No-reference blur estimation based on the average cone ratio in the wavelet domain. Proceedings of SPIE, 2011, , .	0.8	Ο
200	Real-time detection of traffic events using smart cameras. , 2012, , .		0
201	Exploring contour and texture features for context-aware patch-based inpainting. , 2013, , .		Ο
202	Three-dimensional quantitative microwave imaging of realistic numerical breast phantoms using Huber regularization. , 2013, 2013, 5135-8.		0
203	Vehicle classification for road tunnel surveillance. Proceedings of SPIE, 2013, , .	0.8	Ο
204	Bayesian demosaicing using gaussian scale mixture priors with local adaptivity in the dual tree complex wavelet packet transform domain. , 2013, , .		0
205	3D quantitative microwave imaging from sparsely measured data with Huber regularization. , 2014, , .		Ο
206	Shearlet-domain task-driven post-processing and filtering of CT noise. Proceedings of SPIE, 2015, , .	0.8	0
207	Exploiting the low-rank property of hyperspectral imagery: A technical overview. , 2016, , .		Ο
208	Image Inpainting and Demosaicing via Total Variation and Markov Random Field-Based Modeling. , 2018, ,		0
209	Image defect detection algorithm based on deep learning. IOP Conference Series: Materials Science and Engineering, 2019, 680, 012041.	0.3	Ο
210	MRI Reconstruction Using Markov Random Field and Total Variation as Composite Prior. Sensors, 2020, 20, 3185.	2.1	0
211	Noise Reduction of Video Sequences Using Fuzzy Logic Motion Detection. Lecture Notes in Computer Science, 2005, , 666-673.	1.0	0
212	Passive Error Concealment for Wavelet Coded Images with Efficient Reconstruction of High-Frequency Content. Lecture Notes in Computer Science, 2008, , 13-24.	1.0	0
213	Fuzzy logic-based approach to wavelet denoising of 3D images produced by time-of-flight cameras. Optics Express, 2010, 18, 21548.	1.7	0
214	Multi-coil magnetic resonance imaging reconstruction with a Markov random field prior. , 2019, , .		0
215	Learned BRIEF $\hat{a} \in \hat{a}$ transferring the knowledge from hand-crafted to learning-based descriptors. , 2020, , .		0
216	Intersubband Reconstruction of Lost Low Frequency Coefficients in Wavelet Coded Images. , 2008, , 241-253.		0

#	Article	IF	CITATIONS
217	The Impact of Non-uniform Label Noise on the Classification of Hyperspectral Images. , 2021, , .		0
218	Deep image hashing based on twin-bottleneck hashing with variational autoencoders. , 2021, , .		0